Similarity between Positronium-Atom and Electron-Atom Scattering

I. I. Fabrikant
Department of Physics and Astronomy, University of Nebraska, Lincoln, Nebraska 68588-0299, USA

G. F. Gribakin
School of Mathematics and Physics, Queen's University Belfast, Belfast BT7 1NN, Northern Ireland, United Kingdom

(Received 21 February 2014; published 18 June 2014)

We employ the impulse approximation for a description of positronium-atom scattering. Our analysis and calculations of Ps-Kr and Ps-Ar collisions provide a theoretical explanation of the similarity between the cross sections for positronium scattering and electron scattering for a range of atomic and molecular targets observed by S. J. Brawley *et al.* [Science **330**, 789 (2010)].

DOI: 10.1103/PhysRevLett.112.243201 PACS numbers: 34.80.-i, 36.10.Dr

Most of the methods employed in the theory of leptonic and atomic collisions are based on solving the Schrödinger equation with the inclusion of pair lepton-lepton and lepton-nuclear interactions. Although the interactions are well known, for complex projectiles and targets such an approach is computationally very involved. An alternative approach is based on many-body equations involving scattering amplitudes, for example, Faddeev equations [1]. The advantage of this approach is in the possibility of using amplitudes representing highly correlated motion between a part of the projectile and the target. A typical example is the collision of a highly excited (Rydberg) atom with a ground-state atom or a molecule. In this problem the scattering amplitude can be expressed in terms of the amplitudes for electron and ion-core scattering by the ground-state atom [2,3]. This is the idea behind the impulse approximation [4].

Another example is the positronium (Ps) scattering by neutral targets. The Ps atom is easily ionized (i.e., broken up) above the ionization threshold (6.8 eV), and in fact the ionization of Ps is becoming the dominant process in Ps-atom collisions at collision energies above about 20 eV [5]. The Ps ionization energy is much smaller than the ionization energies of the noble-gas atoms and many small molecules (such as H_2, N_2, O_2, CO_2, or SF_6). This allows us to consider the Ps atom as a loosely bound system and the Ps-atom (molecule) scattering as a coherent superposition of e^--atom and e^+-atom scattering processes.

Recently observed similarities between the Ps scattering and the electron scattering from a number of atoms and molecules [6,7] suggest that both processes are largely controlled by the same interactions. When plotted as a function of the projectile velocity, the electron and Ps cross sections are very close and even show similar resonance-like features. This seems strange at first since in the electron-atom scattering the electrostatic and polarization forces play a role, while both seem to be absent in the Ps-atom scattering. However, at intermediate energies electron scattering by noble-gas atoms is dominated by a strong exchange interaction. There is a range of energies above the Ramsauer minimum for the e^--atom scattering, where the polarization is less significant, but the energy is still not too high, so that e^- or e^+ Rutherford scattering is not dominant. In this energy range electron scattering by atoms and molecules is strongly affected by the exchange interaction whereas the positron scattering is relatively weak because of the mutual cancellation of the repulsive static and attractive polarization forces. As a result, in the intermediate energy range, typically between about 5 and 50 eV, positron scattering cross sections are significantly smaller than their electron counterparts [8,9].

Close-coupling calculations of Blackwood *et al.* [10] produced total cross sections for Ps scattering by noble-gas atoms that are substantially lower than the corresponding electron scattering cross sections, and lie below the experimental values [5–7]. These calculations allowed for the distortion and breakup of Ps, but they were performed in the frozen-target approximation; i.e., they did not take into account virtual excitation of the target. In low-energy electron- and positron-atom collisions such virtual excitations can be described in terms of the polarization interaction, and are known to be important. For low-energy Ps-atom collisions they give rise to the van der Waals interaction. In the intermediate-energy range above the Ps excitation threshold, which we are interested in, the static van der Waals interaction is not appropriate for the description of dynamical correlations between the Ps and the target. The most direct way to include them for Ps-atom scattering is by extending the close-coupling calculations to account for the virtual excitations of the target. While such calculations have been performed for Ps collisions with the H atom [11,12] and would be an ultimate goal in the problem of Ps-atom collisions, in the present Letter we demonstrate that a much simpler method based on the impulse approximation can account for dynamical correlations, at least in the intermediate energy range important for the experiments [6,7,13]. This

method also offers a theoretical explanation for the similarity between electron-atom and Ps-atom scattering.

Consider the scattering process

$$\mathrm{Ps}(a,\mathbf{p}_i)+A\rightarrow\mathrm{Ps}(b,\mathbf{p}_f)+A,$$

where a and $\mathbf{p}_i$ denote the internal state and center-of-mass momentum of the incident Ps, while b and $\mathbf{p}_f$ are their values in the final state.

Compared with noble-gas atoms, the Ps is a diffuse and weakly bound system. Consequently, we can assume that when the Ps is scattered off such targets, the Coulomb interaction within the Ps atom is weak in comparison with the electron-atom or positron-atom interactions. In this case the scattering amplitude can be approximated by the sum of two contributions shown schematically in Fig. 1.

Each of the two diagrams in Fig. 1 is in fact a perturbation-theory sum which includes the electron-atom or positron-atom interaction to all orders. Owing to the diffuse nature of Ps and low relative velocities inside Ps, the particle which does not interact with the target (i.e., the positron in the first diagram, and the electron in the second diagram in Fig. 1) does not change its instantaneous momentum. We assume that the state of atom A does not change during the collision. However, the virtual excitations of the target are accounted for implicitly in the electron and positron scattering amplitudes if they are calculated beyond the static (or static-exchange) approximation. As a result, the Ps-atom scattering amplitude can be written as the sum of two terms [3,14] (in atomic units),

$$f_{ba}(\mathbf{p}_f,\mathbf{p}_i)=2\int g_b^*(\mathbf{q})f^-(\mathbf{v}_f^-,\mathbf{v}_i^-)g_a(\mathbf{q}+\Delta\mathbf{p}/2)d^3\mathbf{q}+2\int g_b^*(\mathbf{q})f^+(\mathbf{v}_f^+,\mathbf{v}_i^+)g_a(\mathbf{q}-\Delta\mathbf{p}/2)d^3\mathbf{q}\,, \tag{1}$$

where $\Delta\mathbf{p}=\mathbf{p}_f-\mathbf{p}_i$ is the change in the Ps momentum, $g_a(\mathbf{q})=(2\pi)^{-3/2}\int e^{i\mathbf{q}\cdot\mathbf{r}}\varphi_a(\mathbf{r})d^3\mathbf{r}$ is the Ps internal wave function in the momentum space ($\mathbf{r}=\mathbf{r}_{e^+}-\mathbf{r}_{e^-}$ being the relative position vector), the factor 2 is due to the Ps mass, and $f^\pm(\mathbf{v}',\mathbf{v})$ are the positron-atom and electron-atom scattering amplitudes for the initial and final velocities

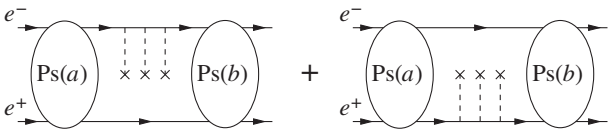

FIG. 1. Schematic diagrams of the approximation for the Ps-atom scattering amplitude. The dashed lines with a cross show the interaction between the electron or positron and the atom, which is included in all orders.

$$\mathbf{v}_i^\pm=\mathbf{p}_i/2-\Delta\mathbf{p}/2\pm\mathbf{q},\qquad \mathbf{v}_f^\pm=\mathbf{p}_i/2+\Delta\mathbf{p}/2\pm\mathbf{q}. \tag{2}$$

The amplitudes $f^\pm$ in Eq. (1) are off the energy shell in the sense that $|\mathbf{v}_i^\pm|\neq|\mathbf{v}_f^\pm|$. Besides, each amplitude depends on the energy argument $E^\pm=\mathbf{p}_i^2/4+\varepsilon_a-|\mathbf{v}_i^\pm|^2/2$ not equal to physical energy $|\mathbf{v}_i^\pm|^2/2$ [2,15]. In order to employ the physical scattering amplitude, we perform the on-shell reduction following Starrett *et al.* [14] and assume that each amplitude is a function of the effective velocity $v^\pm=\max(v_i^\pm,v_f^\pm)$ and momentum transfer $s=|\Delta\mathbf{p}|$ linked to the scattering angle $\theta^\pm$ by $s=2v^\pm\sin(\theta^\pm/2)$.

In view of what was said about the importance of the exchange interaction between the electron and the target, let us first neglect the positron contribution to the amplitude (1). The total differential cross section for scattering from the state a can then be written as

$$\frac{d\sigma_a}{d\Omega}=4\sum_b\frac{v_b}{v_a}\int g_b^*(\tilde{\mathbf{q}})g_b(\mathbf{q})[f^-(\tilde{v}^-,s)]^*f^-(v^-,s)g_a^*(\tilde{\mathbf{q}}+\Delta\mathbf{p}/2)g_a(\mathbf{q}+\Delta\mathbf{p}/2)d^3\mathbf{q}d^3\tilde{\mathbf{q}},$$

where v_a and v_b are the Ps velocities in the initial and final states. We will assume now that the collision energy is well above a typical Ps excitation threshold, so that we can neglect the dependence of v_b and the momentum transfer $\Delta\mathbf{p}$ on b. Then the sum over b yields $\delta(\mathbf{q}-\tilde{\mathbf{q}})$ and we obtain

$$\frac{d\sigma_a}{d\Omega}=4\int|f^-(v^-,s)|^2|g_a(\mathbf{q}+\Delta\mathbf{p}/2)|^2d^3\mathbf{q}. \tag{3}$$

If the state a is the ground state of Ps, the function $|g_a|^2$ in Eq. (3) exhibits a sharp peak at $\mathbf{q}+\Delta\mathbf{p}/2\approx0$, and can be replaced by the δ function in the "peaking approximation" [16]. Equation (2) then gives $\mathbf{v}_i^-\approx\mathbf{p}_i/2=\mathbf{v}_i$ and $\mathbf{v}_f^-\approx\mathbf{v}_i+\Delta\mathbf{p}$, where $\mathbf{v}_i$ is the incident Ps velocity. Thus, we can neglect the variation of $f^-(v^-,s)$ when integrating over $\mathbf{q}$ in Eq. (3), and obtain

$$\frac{d\sigma_a}{d\Omega}=4|f^-(v^-,s)|^2.$$

For calculation of the integral cross section we note that the Ps and electron solid angles are related by $d\Omega=d\Omega^-/4$, which gives

$$\sigma_a(\mathrm{Ps})=\sigma_a(e^-). \tag{4}$$

Hence the total integral cross sections for Ps-A and e^--A collisions are equal for equal incident *velocities* $v^-\approx v_i$.

In deriving this result we made several approximations, assuming that the collision energy is high compared to the typical Ps excitation energy and that the e^--A interaction dominates Ps-A collisions. The latter assumption is

supported by experiments and calculations showing that for scattering from noble-gas atoms in the intermediate energy range ($v = 0.5$–2 a.u.) the e^+-A collision cross sections are much smaller than the e^--A cross sections (see, e.g., [17,18] and [8] for molecules). In contrast, at low energies (< 1 eV) the e^+-A cross sections are larger due to the effect of virtual Ps formation [9,19], leading to larger absolute values of the scattering lengths.

We will present now the results for the partial and total cross sections of Ps-Kr and Ps-Ar scattering obtained by full three-dimensional integration in Eq. (1). The scattering phase shifts necessary for the calculation of the electron and positron scattering amplitudes are taken from polarized-orbital calculations of McEachran *et al.* [20–23]. Note that many calculations of e^+ collisions with Ar and Kr have been published after the work of McEachran *et al.* (see, e.g., Ref. [24] and references therein), some at a more advanced level. However, our goal in the present work is to demonstrate the correspondence between e^--A and Ps-A scattering, and Refs. [20–23] are most convenient for this purpose since they present the scattering phase shifts calculated consistently for all four cases (e^--Ar, e^+-Ar, e^--Kr, and e^+-Kr).

In the present work we have calculated the amplitudes and cross sections for Ps elastic scattering and excitation of $n = 2$ states of Ps. To obtain the total cross section, the Ps ionization (i.e., breakup) contribution should be added. This was taken from the calculations of Starrett *et al.* [14] for the velocity range between the ionization threshold ($v = 0.5$ a.u.) and $v = 1.7$ a.u. For higher velocities we use a smooth extrapolation.

Figure 2 shows the cross sections for Kr, plotted as functions of the velocity of the projectile (e^-, e^+, and Ps). Cross sections for e^+ at $v > 1.3$ a.u. were obtained by extrapolation of the scattering phase shifts of McEachran *et al.* [21]. By using different extrapolation schemes, we have estimated the uncertainty of the cross sections at $v > 1.3$ a.u. to be less than 5%. The Ps-Kr elastic cross section dominates the total below the ionization threshold at $v = 0.5$ a.u., but above this velocity the ionization contribution is substantial and becomes comparable to the elastic cross section above $v = 0.7$ a.u. As a result of the rise in the ionization contribution, the total cross section exhibits a weak maximum at $v = 0.8$ a.u., much flatter than that in the e^--Kr cross section, mainly because the Ps elastic cross section grows rapidly towards lower energies. This growth is mostly due to the e^+ contribution to the amplitude (1). In contrast, for velocities above 0.5 a.u., e^--Kr scattering dominates, and the total Ps-Kr cross section approaches that of e^--Kr scattering.

Comparison with the elastic cross section from the static-exchange calculations of Blackwood *et al.* [10] shows agreement with our Ps-Kr elastic cross section for $v = 0.5$–1 a.u. The impulse approximation is not expected to work at low collision energies below the Ps ionization

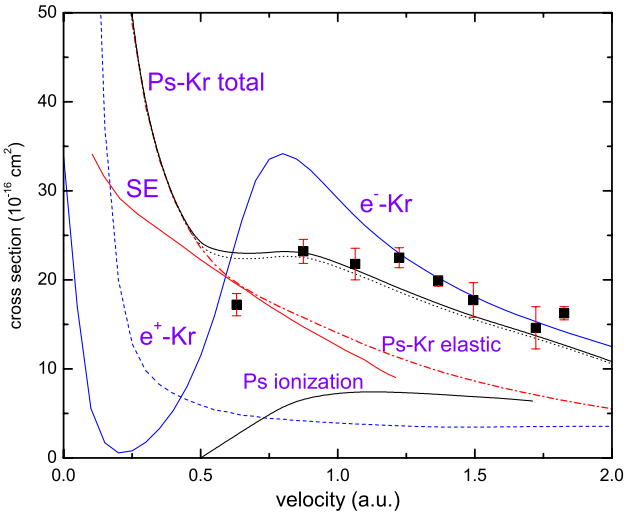

FIG. 2 (color online). e^--Kr, e^+-Kr, and Ps-Kr scattering cross sections. Dotted black line is the sum of the elastic and ionization [14] cross section, and the line "Ps-Kr total" also contains contribution from excitation of the $n = 2$ levels of Ps. Solid red line "SE" is the elastic cross section from static-exchange calculations of Blackwood *et al* [10]. Experimental data with error bars are from Ref. [6], and the data for e^--Kr and e^+-Kr scattering are from Refs. [21,23].

threshold which suggests that the sharp upturn of the cross section below $v = 0.5$ a.u. is an artifact. Instead the cross section should approach the zero-energy limit of Mitroy and Bromley [25] $\sigma = (6$–$24) \times 10^{-16}$ cm^2 calculated by the stochastic variational method. (The numbers indicate the bounds due to uncertainty in the input parameters of their model.) It is somewhat surprising that our results remain in good agreement with the static-exchange calculations [10] down to the velocity 0.3 a.u. We should note, though, that because of the frozen-target approximation, the van der Waals interaction is not effectively included in calculations [10], and in the case of Ps-H scattering it was shown by the same group [11,12] that inclusion of virtual excitations of Ps and the target leads to much smaller cross sections in the low-energy region. Note also that the Ps excitation cross section is very small compared to elastic and ionization, in agreement with Blackwood *et al.* [10].

Note that in order to obtain a peak in the total Ps cross section, adding the inelastic contribution, mainly ionization cross section for Ps, is crucial. As a result, our total Ps-Kr scattering cross sections agree well with the measurements of Brawley *et al.* [6], although, in contrast to observations, the calculated peak is very weak, and looks more like an inflection point due to failure of the impulse approximation at low energies.

In Fig. 3 we present the results for Ar. Since the Ps excitation cross sections are very small compared to elastic scattering, we include only elastic and ionization contributions in the total. The major features in the elastic and total cross sections are the same as for Kr, and the peak at

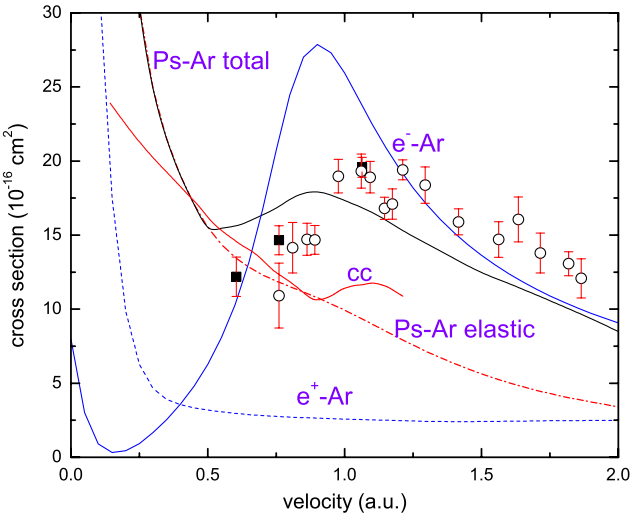

FIG. 3 (color online). e^--Ar, e^+-Ar, and Ps-Ar scattering cross sections. The solid line "Ps-Ar total" contains contribution of the elastic scattering calculated from Eq. (1) and ionization (from Ref. [14]). Solid red line "cc": elastic cross sections from close-coupling calculations [10]. Circles with error bars: experiment [13]. Squares with error bars: experiment [6]. The data for e^+-Ar and e^--Ar scattering are from [20,22]. Cross sections for e^+ at $v > 1.3$ a.u. were obtained by extrapolation of the scattering phase shifts of McEachran *et al.* [20].

$v = 0.9$ a.u. in the total cross section is more pronounced. The elastic cross section is close to the results of the frozen-target close-coupling calculations [10] for $v = 0.5$–0.8 a.u. (where the latter is dominated by elastic scattering), and the total agrees well with the experiment [6,13]. However, as in the case of Kr, the upturn below $v = 0.5$ a.u. is an artifact of the impulse approximation. Most likely, the cross section below this velocity should approach the zero-energy limit of Mitroy and Ivanov [26], $\sigma = (7\text{–}16) \times 10^{-16}$ cm^2. The sharp upturn in the Ps scattering cross section at low velocities is due to the contribution of the e^+-Ar scattering amplitude. When this contribution is neglected, the low-energy Ps scattering cross section becomes substantially lower and falls within the Mitroy-Ivanov boundaries. The same is true for the Ps-Kr scattering. It is not clear whether this result is fortuitous or physically significant.

In conclusion our work offers a clear physical and quantitative theoretical explanation for the unexpected similarity between the Ps and electron scattering for equal projectile velocities uncovered recently by experiment [6,7]. Physically, this phenomenon occurs due to the relatively weak binding and diffuse nature of Ps, and the fact that electrons scatter more strongly than positrons off atomic targets for incident velocities $v \sim 1$ a.u. Such similarity appears to be a generic phenomenon, and it is natural that an explanation is offered by using an approximation (in this case, impulse approximation) which emphasizes the physics of the problem. By contrast, large-scale numerical calculations for specific targets may be capable of reproducing experimental data but often lack the transparency required for providing physical insight. Note that the present impulse-approximation approach can also be improved by extension of the e^--A and e^+-A scattering amplitudes off the energy shell and by considering higher-order approximations of the Faddeev theory [15,27].

The authors are grateful to G. Laricchia for stimulating discussions and for providing experimental data in numerical form.

[1] L. D. Faddeev, Sov. Phys. JETP **12**, 1014 (1961).
[2] E. de Prunelé, Phys. Rev. A **27**, 1831 (1983).
[3] M. Matsuzawa, J. Phys. B **17**, 795 (1984).
[4] G. F. Chew and G. C. Wick, Phys. Rev. **85**, 636 (1952).
[5] G. Laricchia and H. R. J. Walters, Riv. Nuovo Cimento Soc. Ital. Fis. **35**, 305 (2012).
[6] S. J. Brawley, S. Armitage, J. Beale, D. E. Leslie, A. I. Williams, and G. Laricchia, Science **330**, 789 (2010).
[7] S. J. Brawley, A. I. Williams, M. Shipman, and G. Laricchia, Phys. Rev. Lett. **105**, 263401 (2010).
[8] M. Kimura, O. Sueoka, A. Hamada, and Y. Itikawa, Adv. Chem. Phys. **111**, 537 (2000).
[9] C. M. Surko, G. F. Gribakin, and S. J. Buckman, J. Phys. B **38**, R57 (2005).
[10] J. E. Blackwood, M. T. McAlinden, and H. R. J. Walters, J. Phys. B **35**, 2661 (2002); **36**, 797 (2003).
[11] C. P. Campbell, M. T. McAlinden, F. G. R. S. MacDonald and H. R. J. Walters, Phys. Rev. Lett. **80**, 5097 (1998).
[12] J. E. Blackwood, M. T. McAlinden, and H. R. J. Walters, Phys. Rev. A **65**, 032517 (2002).
[13] A. J. Garner, A. Özen, and G. Laricchia, J. Phys. B **33**, 1149 (2000).
[14] C. Starrett, M. T. McAlinden, and H. R. J. Walters, Phys. Rev. A **72**, 012508 (2005).
[15] I. I. Fabrikant, Phys. Rev. A **45**, 6404 (1992).
[16] J. S. Briggs, J. Phys. B **10**, 3075 (1977).
[17] W. E. Kauppila, T. S. Stein, J. H. Smart, M. S. Dababneh, Y. K. Ho, J. P. Downing, and V. Pol, Phys. Rev. A **24**, 725 (1981).
[18] M. S. Dababneh, Y.-F. Hsieh, W. E. Kauppila, V. Pol, and T. S. Stein, Phys. Rev. A **26**, 1252 (1982).
[19] V. A. Dzuba, V. V. Flambaum, G. F. Gribakin, and W. A. King, J. Phys. B **29**, 3151 (1996).
[20] R. P. McEachran, A. G. Ryman, and A. D. Stauffer, J. Phys. B **12**, 1031 (1979).
[21] R. P. McEachran, A. D. Stauffer, and L. E. M. Campbell, J. Phys. B **13**, 1281 (1980).
[22] R. P. McEachran and A. D. Stauffer, J. Phys. B **16**, 4023 (1983).
[23] R. P. McEachran and A. D. Stauffer, J. Phys. B **17**, 2507 (1984).
[24] L. A. Poveda, A. Dutra, J. R. Mohallem, and D. Assafrão, Phys. Rev. A **87**, 052702 (2013).
[25] J. Mitroy and M. W. J. Bromley, Phys. Rev. A **67**, 034502 (2003).
[26] J. Mitroy and I. A. Ivanov, Phys. Rev. A **65**, 012509 (2001).
[27] D. B. Khrebtukov and I. I. Fabrikant, Phys. Rev. A **51**, 4675 (1995).